Journal of NeuroVirology, 16: 125–132, 2010

ISSN 1355-0284 print / 1538-2443 online
DOI: 10.3109/13550281003682521

informa
healthcare

Lipopolysaccharide treatment and inoculation of influenza A virus results in influenza virus–associated encephalopathy–like changes in neonatal mice

Tomohisa Tanaka,[1] Yuji Sunden,[1] Yoshihiro Sakoda,[2] Hiroshi Kida,[2] Kenji Ochiai,[1] and Takashi Umemura[1]

[1]Laboratorie of Comparative Pathology; and [2]Laboratory of Microbiology, Graduate School of Veterinary Medicine, Hokkaido University, Sapporo, Japan

Influenza virus–associated encephalopathy (IAE) is a highly mortal neural complication of influenza A virus (IAV) infection, mostly affecting children younger than 5 years old, and the brain pathology of IAE is characterized by peracute brain edema with evidence of an impaired blood-brain barrier. The pathogenesis of IAE is unknown, but hypercytokinemia of tumor necrosis factor (TNF)-α, interleukin (IL)-1β, and IL-6 is suspected of playing a central role in the development of IAE. Because the brain pathology of IAE is similar to that of septic encephalopathy due to endotoxemia, the effect of combined treatment of IAV and lipopolysaccharide (LPS) was tested using suckling mice. The results show that pulmonary infection with non-neurotropic IAV enhanced the neuropathogenicity of LPS and induced encephalopathy that was similar to IAE with respect to the occurrence of central nervous system (CNS) histopathology and the absence of direct infection of IAV in the brain. Influenza A virus also increased blood-brain barrier (BBB) permeability and induced inflammatory cytokines in the blood. These results suggested that the mice treated with IAV+LPS are possible animal models of IAE, and that hypercytokinemia and/or the involvement of endotoxemia in IAV infection are possible causes of IAE. *Journal of NeuroVirology* (2010) **16,** 125–132.

Keywords: encephalopathy; inflammatory cytokines; influenza virus; mouse model

Introduction

Influenza virus-associated encephalopathy (IAE) is a rare but highly mortal neural complication of influenza virus infection, mostly affecting children younger than 5 years old (Morishima *et al*, 2002). It has been reported around the world (Toovey, 2008), but patients have been found most frequently in Japan. According to etiological research, IAE is typically associated with non-neurotropic H3N2 influenza A virus (IAV) infection (Morishima *et al*, 2002). Postmortem microscopic analyses on the patients demonstrated hyalinization of blood vessels and extravascular leakage of plasma proteins in the brains, which suggest the occurrence of vasogenic edema due to damage of vascular endothelial cells (Morishima *et al*, 2002). The encephalopathy is often followed by disseminated intravascular coagulation and multiple organ failure (Togashi *et al*, 2004; Yokota *et al*, 2000).

The pathological mechanism of the IAE is unknown. In IAE patients, IAV infects mucosal epithelial cells of the respiratory tract, and an isolation of the virus from the central nervous system (CNS), including the cerebrospinal fluid (CSF), is usually negative (Ito *et al*, 1999; Smidt *et al*, 2004). Therefore, the direct invasion of the virus into the CNS is irrelevant as the cause of IAE. Miniplasmin, a hemagglutinin processing protease, accumulates in the cerebral capillaries of mice with abnormal

Address correspondence to Takashi Umemura, Laboratory of Comparative Pathology, Graduate School of Veterinary Medicine, Hokkaido University, N18 W9, Kita-ku, Sapporo 060-0818, Japan. E-mail: umemura@vetmed.hokudai.ac.jp.
This study was supported by Grants-in-Aid for Scientific Research from the Ministry of Education, Culture, Sports, Science, and Technology, Japan.

Received 6 October 2009; revised 26 November 2009; accepted 8 January 2010.

mitochondrial β-oxidation after non-neurotropic IAV infection (Yao *et al*, 2004). The accumulation of miniplasmin allows non-neurotropic IAV to infect the cerebral vascular endothelial cells, which triggers the increased permeability of the blood-brain barrier (BBB). However, it may not be the cause of IAE, since IAV has not usually been demonstrated in the CNS of IAE patients and this animal model is accompanied by a fatty change in hepatocytes similar to Reyes' syndrome (Okita *et al*, 1996). Elevated concentrations of several cytokines, including tumor necrosis factor (TNF)-α, soluble TNF receptor 1, interleukin (IL)-6, and IL-1β, have been reported in the serum and CSF of IAE patients (Ichiyama *et al*, 2003; Ito *et al*, 1999), and the concentrations of these inflammatory cytokines were correlated with the severity of CNS dysfunction (Aiba *et al*, 2001; Toovey, 2008). From these results, hypercytokinemia is suspected of playing an important role in the development of IAE. However, there are arguments on whether the hypercytokinemia is the cause or result of IAE, since the involvement of hypercytokinemia to IAE has not been experimentally confirmed yet and the direct cause of hypercytokinemia in IAE is unknown.

Sepsis is a condition characterized by uncontrolled bacterial infection and affects many organs, including the CNS. Septic encephalopathy is one of the common complications of sepsis and is characterized by diffuse or multifocal neural dysfunction as a result of an inflammatory response with or without direct bacterial invasion into the brain (Papadopoulos *et al*, 2000). Administration of lipopolysaccharide (LPS), a structural component of the outer membrane of gram-negative bacteria, induces pathological changes that mimic the process of sepsis (Alexander *et al*, 2008; Papadopoulos *et al*, 2000). The predominant microscopic findings of the encephalopathy are vasogenic cerebral edema and neuronal damage (Bogdanski *et al*, 2000; Stolp *et al*, 2005). Although the mechanism of septic encephalopathy is not fully elucidated, TNF might play an important role in the pathogenicity (Alexander *et al*, 2008). Therefore, septic encephalopathy is similar to IAE regarding the involvement of inflammatory cytokines as well as the CNS histopathology.

In this study, we demonstrate that pulmonary infection of non-neurotropic IAV enhances neuropathogenicity of LPS and induces encephalopathy similar to IAE in regards to the occurrence of CNS histopathology with the absence of direct infection of IAV in the brain, an increase of BBB permeability, and the induction of inflammatory cytokines in the blood.

Results

General statuses and survival rates of each group of mice

We gave inoculations of IAV, LPS, or both (IAV+LPS) to 1-week-old ICR mice. The mice of the IAV group showed depression, rough fur, and emaciation at 3 to 4 days post infection (dpi), which progressively worsened. Meanwhile, LPS and IAV+LPS group mice showed similar symptoms as well as diarrhea and a sluggish response to manual stimulations within several hours of the LPS inoculations. The general symptoms appeared severer in the IAV+LPS group than in the LPS group. All the mice in the LPS group survived, whereas 93% and 68% of mice in the IAV and IAV +LPS groups survived, respectively (Figure 1).

Histopathological changes in mice

The mice of the IAV and IAV+LPS groups showed multifocal bronchointerstitial pneumonia in the lungs (Figure 2A). The lesions were mainly located around the bronchioles, and the bronchiolar and alveolar walls were thickened by infiltration of mononuclear cells and neutrophils. Bronchiolar lumina and alveoli also contained a small number of sloughed epithelial cells. There were no obvious differences between the mice in the IAV and IAV +LPS groups regarding the quality, distribution, and severity of the pulmonary lesions. Although there were no any significant lesions in the brains of the IAV group, multifocal microbleeding, irregular dilation of perivascular spaces, and neutrophilic infiltration were found in the brains of the mice in the LPS and IAV+LPS groups (Figure 2B, C). These brain lesions were usually located at the cerebral cortex and brain stem, and were sometimes accompanied by mild spongiform change of neuropils and Alzheimer type 2–like degenerated astrocytes (Figure 2D). These cerebral lesions appeared 24 h after the second inoculation of LPS, and were more prominent in the IAV+LPS group than the LPS group 48 h after this inoculation. Other organs were unremarkable, except that there was a depletion of thymic lymphocytes in the LPS and IAV+LPS groups. There were no significant differences in the histopathological semiquantitative scores on thymic lymphocytic depletion and bronchointerstitial pneumonia between IAV and IAV +LPS groups. Cerebral lesions in the IAV+LPS group were more severe than those in the LPS group,

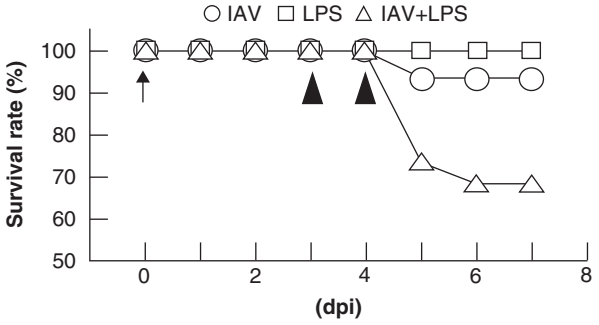

Figure 1 Survival rates of IAV, LPS, and IAV+LPS group mice. The mice were inoculated with IAV (IAV and IAV+LPS groups) or saline (LPS group) at 0 dpi (arrow). Then, the mice received inoculations of LPS (LPS and IAV+LPS mice) or saline (IAV mice) at 3 and 4 dpi (arrow heads).

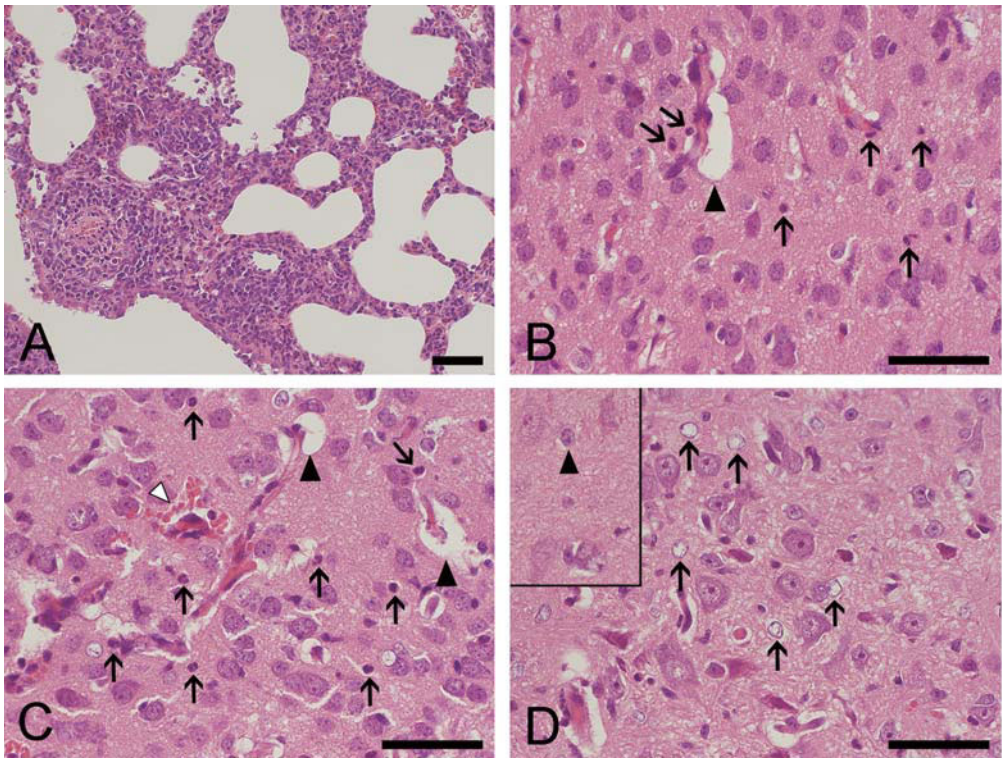

Figure 2 Representative histopathology of the lungs (**A**) and brain (B-D) from IAV+LPS group mice at 5 dpi. (A) Bronchointerstitial pneumonia due to IAV infection. (**B**) Cerebral microbleeding (arrowhead) and irregular dilation of perivascular spaces (arrows). (**C**) Neutrophils (arrows) infiltrating the cerebral cortex. (**D**) Mild spongiform change of neurophil and degenerated astrocytes having vacuolated and swollen nuclei. Hematoxylin and eosin stain. Bars = 50 μm.

especially regarding the severity of cerebral microbleeding (Table 1).

The estimation of cerebrovascular permeability

To evaluate cerebrovascular permeability, we administered Evans blue (EB) dye to the abdominal cavity of mice, and then compared the concentration of the dye in the brains from the IAV, LPS, and IAV+LPS groups. Taken as a whole, the color of the brains from the IAV group was normal, whereas the brains from the LPS and IAV+LPS groups had a noticeable bluish tinge that appeared deeper in the IAV+LPS group than in the LPS group (Figure 3A). To quantify the concentrations of EB dye, the densities of the dye in the brains were measured by absorption spectrometry (Figure 3B). The brains from the IAV+LPS group contained significantly higher levels of the dye than those from the LPS group. These results suggest that the integrity of the BBB significantly deteriorated in the IAV+LPS group, and the results were consistent with histopathological data in which the mice of the IAV+LPS group showed severer cerebral lesions than the other groups.

The induction of cytokines in plasma

In previous studies, it has been reported that the infection of IAV enhanced the inductions of inflammatory cytokines in human leukocytes (Lundemose *et al*, 1993; Nain *et al*, 1990), and inflammatory cytokines were demonstrated to have important roles

Table 1 Scores of microscopic changes

Groups	Time since 2nd LPS injections	Thymus Lymphocytic depletion	Lungs Interstitial pneumonia	Brain		
				Microbleeding	Neutrophilic infiltration	Edema
IAV		0 (0–0)[a]	2 (2–2)	0 (0–0)	0 (0–0)	0 (0–0)
LPS	48 h	2 (1.25–2)	0 (0–0)	1.5 (1–2)	2.5 (1.25–3)	2 (1.25–2)
	72 h	2 (2–2)	0 (0–0)	0 (0–0)	2 (1.5–2)	2 (0.5–2)
IAV+LPS	48 h	3 (3–3)	1.5 (1–2)	3 (3–3)*	3 (3–3)	2 (2–3)
	72 h	2 (1.5–2)	2 (2–2)	0 (0–0)	2 (1.5–2)	1 (1–1.5)

[a]Values mean median of scores (25–75 percentile) in this order. 0 = no obvious change; 1 = focal mild change; 2 = multifocal moderate change; 3 = diffuse, moderate to severe change. *$P < .05$. Differences were analyzed using Mann-Whitney U test.

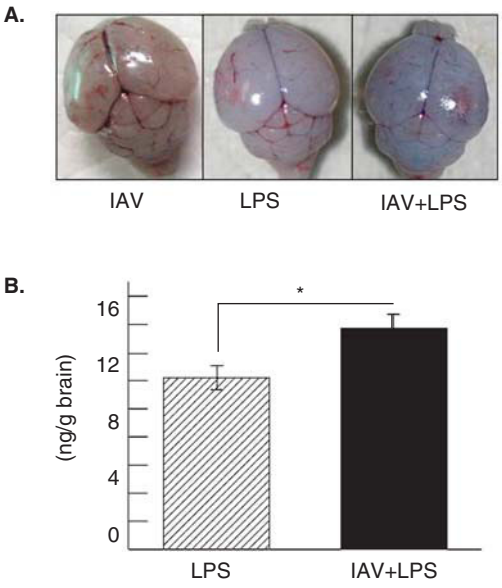

Figure 3 Comparison of BBB integrity. (**A**) Photographs of the brains from the IAV, LPS, and IAV+LPS groups injected intraperitoneally with EB dye. The brains were collected after 48 h of LPS inoculations. (**B**) Quantification of EB dye extracted from the brains. Each error bar means standard error. The statistical comparison was performed using Student's *t* test (*$P < .05$).

as pathogenic agents of LPS (Alexander *et al*, 2008; Papadopoulos *et al*, 2000). Therefore, we measured the levels of plasma cytokines in order to clarify whether IAV infection affects the inductions of inflammatory cytokines by LPS as well as the severity of the encephalopathy. Cytokine levels in the plasma of each group were measured 6, 12, and 24 h after the LPS inoculations. Six hours after the LPS inoculations, the induction of most inflammatory cytokines was upgraded in the LPS and IAV +LPS groups (Figure 4A–D). The serum concentrations of TNF-α and IL-6 in the IAV+LPS group were significantly higher than those in the IAV and LPS groups (Figure 4A, C). In addition, the concentrations of monocyte chemoattractant protein (MCP)-1 and IL-10 in the IAV+LPS group were significantly higher than those in the IAV group (Figure 4B, D). In contrast, the interferon (IFN)-γ level of the IAV group tended to be higher without statistical significance than those of the other groups (Figure 4E). The high cytokine levels in the LPS and IAV+LPS groups dropped to normal or to lower levels than normal until 24 h after of the LPS stimulations (data not shown). Serum concentrations of IL-12p70 were unchanged in all groups throughout the experiments (data not shown).

The distribution of viral antigens and viral titer measurement

Viral antigens were detected by immunohistochemistry in the lungs from IAV and IAV+LPS groups. The IAV antigens were located in bronchiolar epithelial cells and alveolar epithelial cells (Figure 5A). In the bronchioli, many bronchiolar epithelial cells showed positive reaction along the walls, and alveolar

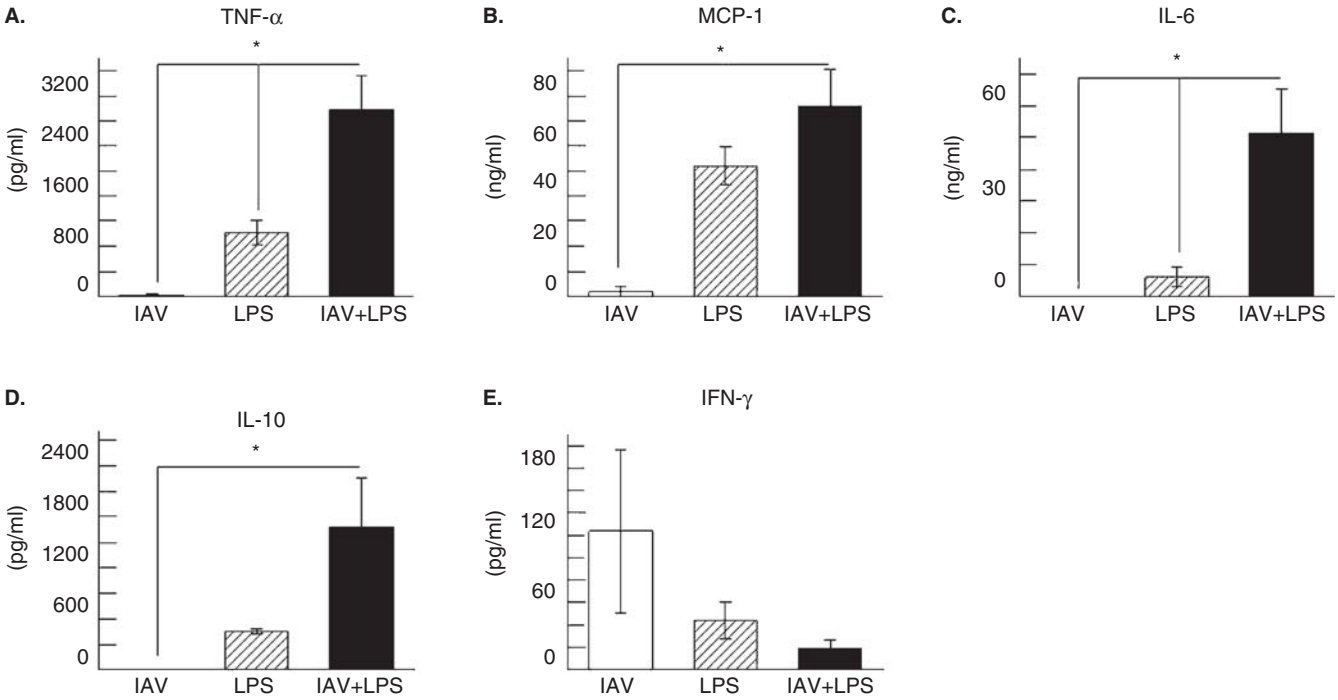

Figure 4 Quantitative analysis of the production of TNF-α (**A**), MCP-1 (**B**), IL-6 (**C**), IL-10 (**D**), and IFN-γ (**E**) in plasma from the IAV, LPS, and IAV+LPS groups. The plasma was collected after 6 h of LPS (or saline) inoculations. Each error bar means standard error. Differences among means were statistically analyzed using Tukey-Kramer multiple comparison tests (*$P < .01$).

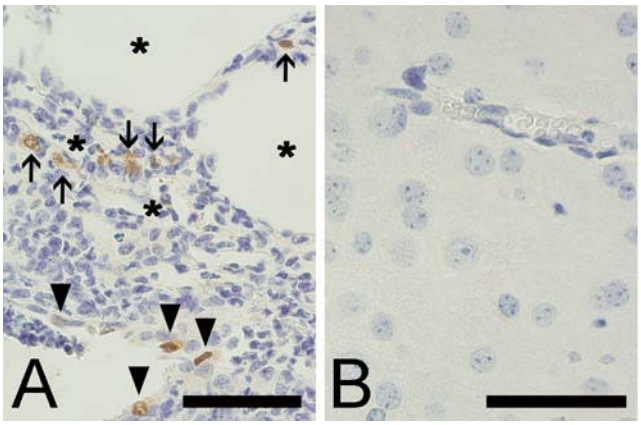

Figure 5 Representative photographs of immunohistochemistry for IAV antigens. (**A**) In the lung from the IAV+LPS group mouse, some bronchiolar and alveolar epithelial cells show positive reactions (arrows). (**B**) The brain of the IAV+LPS mouse is entirely negative for virus antigen. The tissues were collected at 5 dpi of LPS. Bars = 50 μm.

epithelial cells which had oval or flattened shapes showed positive reaction in some thickened alveolar walls. There were no obvious differences in the localization and amounts of the antigen between both groups. However, organs such as the liver, spleen, kidneys, heart, and brain (Figure 5B) stained negative for IAV antigens in the IAV and IAV+LPS groups. We measured viral titers of the lungs and brain by plaque assay. Viral titers in the lungs of the IAV and IAV+LPS groups were 6.62 ± 0.08 and 6.42 ± 0.13 (mean ± SEM: $\log_{10}$ plaque-forming units [PFU]/g), respectively. IAV was not isolated from brain of the IAV and IAV+LPS groups by plaque assay.

Discussion

Early diagnosis, prevention, and therapy for IAE are still to be established because the pathological mechanisms of the disease are unknown. The disease usually occurs in children younger than 5 years of age, and we used neonatal mice to produce IAE in the present experiment. IAV infection induced bronchointerstitial pneumonia in neonatal mice with survival rate of 93% in the IAV group. There were no differences in the viral titers and localization of viral antigen between the IAV and IAV+LPS groups. Survival rates of the IAV+LPS and LPS groups were 68% and 100%, respectively, and only the CNS involvement was severer in the IAV +LPS group than the LPS group. Therefore, the CNS damage was considered to be the direct cause of the decreased survival rate in the IAV+LPS group.

The microscopic cerebral lesions, including microbleeding and dilation of perivascular space, suggest the impairment of cerebral blood vessels and vasogenic edema. This was consistent with the findings of LPS-induced encephalopathy in previous reports (Bogdanski *et al*, 2000; Stolp *et al*, 2005). Scattered neutrophilic infiltration was likely to be the secondary reaction to the brain damage. In our experiment, IAV infection aggravated LPS-induced encephalopathy. Similarly, an infection of infant ferrets with IAV enhanced their susceptibility to the lethal effects of endotoxin (Jakeman *et al*, 1991). The pathological mechanism of LPS encephalopathy remains to be elucidated, but previous studies reported the participation of multiple factors, including inflammatory cells and their mediators, reduced cerebral blood flow, and disruption of the BBB (Papadopoulos *et al*, 2000). In the present study, we did not find any intravascular thrombi in all mice and it was unlikely that microvascular infarction caused cerebral damage in the LPS and IAV+LPS groups. On the other hand, IAV infection enhanced an increase of BBB permeability and the production of TNF-α and IL-6 in plasma of the IAV+LPS mice. The enhanced TNF-α induction may contribute to cerebral vascular damage because TNF-α has a critical role as a pathogenic agent of LPS-induced encephalopathy (Alexander *et al*, 2008). Previous *in vitro* studies using human peripheral blood leukocytes revealed that the production of TNF-α, IL-1, and IL-6 was enhanced by the combined treatment of IAV and LPS (Lundemose *et al*, 1993; Nain *et al*, 1990). Although the mechanism of cytokine induction by IAV and LPS treatment was not elucidated completely, it was suggested that IAV and LPS concurrently activate several common transcription factors responsible for cytokine gene expression, including nuclear factor (NF)-κB, interferon regulatory factor (IRF), and activator protein (AP)-1 (Julkunen *et al*, 2000; Kawai and Akira, 2006). Additionally, LPS is thought to potentiate cytokine synthesis at the posttranscriptional level (Han *et al*, 1990; Nain *et al*, 1990). In the present experiment, the level of plasma TNF-α and the severity of brain lesions were positively correlated. Therefore, the infection of neonatal mice with non-neurotropic IAV might enhance LPS-induced encephalopathy by means of overinduction of cytokines such as TNF-α and IL-6, which contributed to cerebral vascular damage and increased permeability of BBB.

Pathological entity of IAE is vasogenic brain edema due to the damage of vascular endothelial cells without direct invasion of IAV to the brain (Morishima *et al*, 2002). Elevated concentrations of cytokines such as TNF-α and IL-6 may be the cause of the disease (Aiba *et al*, 2001; Ichiyama *et al*, 2003; Ito *et al*, 1999; Toovey, 2008). In the present experiment, IAV+LPS mice showed the IAE-like encephalopathy in respect to the vasogenic brain disorders and the dynamics of plasma inflammatory cytokines without direct infection of IAV to the brain. From these results, it may be concluded that the mice treated with IAV+LPS are a potential animal model of IAE, and that hypercytokinemia and/or the involvement of endotoxemia in IAV infection are possible causes of IAE.

Materials and methods

Virus and mice
Influenza A virus strain A/Aichi/2/68 (H3N2) was propagated in 10-day-old embryonated chicken eggs at 35°C for 48 h (Isoda *et al*, 2006). The virus-containing allantoic fluid was stored at −80°C and used as the source of virus. The infectivity of the virulent fluid was determined using hamagglutinin assay and plaque assay.

Pregnant ICR mice were purchased from Charles River Laboratories Japan (Kanagawa, Japan). The 7-day-old suckling mice were submitted to the following animal experiment. To minimize the difference between maternal mice, the number of neonatal mice was kept around 12 per female mouse. All animal studies were carried out with the approval of the committee of Laboratory Animal Experimentation, Graduate School of Veterinary Medicine, Hokkaido University, and are consistent with the Association for Assessment and Accreditation of Laboratory Animal Care International standards.

Inoculation of influenza virus and LPS to mice
Seven-day-old mice were anesthetized by isoflurane inhalation and inoculated in both nostrils with 10 μl (1×10^5 PFU) of IAV. Then, the mice were inoculated with LPS of *Esherichia coli* O55:B5 (Sigma, St. Louis, MO, USA) twice. Briefly, the mice received 0.5 μg/g of the first LPS injection to the hindlimb muscle at 3 dpi of the virus inoculation, followed by the second injection of 20 μg/g LPS to the peritoneal cavity 24 h after the first injection. Control mice were inoculated with equivalent volumes of sterile saline in place of IAV or LPS. Each mouse was monitored for 7 days, or was submitted to the collection of whole blood under anesthesia and necropsied during 4 to 7 dpi at 6- or 12-h intervals.

Histopathological analysis and semiquantitative evaluation of microscopic changes
At necropsy, tissue samples from the liver, spleen, kidneys, heart, lungs, thymus, and brain were collected from mice, fixed in 20% neutral-buffered formalin solution, and embedded in paraffin wax. The tissue samples were sectioned at a thickness of 4 μm and stained with hematoxylin-eosin stain for light microscopy. Histopathological changes of thymus, lungs, and brains were semiquantitatively scored from score 0 (absent) to score 3 (severe) on the basis of the distribution and severity. Briefly, we made sections from predetermined areas of thymus, lungs and brain. For the evaluation of pulmonary lesion, we obtained four sections from lungs (two sections from the left lung and two sections from the anterior and caudal lobes of the right lung). For the evaluation of brain lesions, we obtained five sections from brain (from each level of frontal lobe, diencephalon, occipital lobe, brain stem, and medulla oblongata). The criteria for scoring were as follows: 0 = no significant lesion; 1 = localized and very mild lesions; 2 = moderate lesions multifocally distributed on more than half of the sections; 3 = moderate to severe lesions diffusely distributed on almost all sections.

Immunohistochemical detection of viral antigen
Serial sections were stained with the streptavidin-biotin immunoperoxidase complex method using Histofine SAB-PO kit (Nichirei, Tokyo, Japan). To restore antigens, the sections were treated with 0.01 M phosphate-buffered saline (PBS) containing 0.1% trypsin (Becton Dickinson, Mountain View, CA, USA) for 20 min at 37°C. As the primary antibody, a diluted rabbit anti-strain A/Whistling swan/Shimane/499/83 (H5N3) hyperimmuno serum (produced in our laboratory) was applied for approximately 12 h at 4°C (Matsuda *et al*, 2004). The chromogenic reaction was performed by 0.05 M Tris-HCl buffer (pH 7.6) containing 0.02% 3,3′-diaminobenzidinetetrahydrochloride (Dojindo Laboratories, Kumamoto, Japan), 0.005% H_2O_2, and 0.01 M imidazole (Sigma). The sections were counterstained with Mayer's hematoxylin. The primary antibody was replaced by 0.01 M PBS for negative controls.

The evaluation of BBB integrity
The integrity of BBB was evaluated by Evans blue (EB; Kanto Chemical, Tokyo, Japan) extravasations, as described previously (Bigdeli and Khoshbaten, 2008; Fukui *et al*, 2003). Briefly, the mice of the IAV group (n = 3), LPS group (n = 4), and IAV +LPS group (n = 4) were injected intraperitoneally with 50 μl of filtered 2% EB solution in sterile saline after 48 h of the second LPS inoculation. The mice were anesthetized after 2 h of EB injection and the brains were rapidly removed. The EB dye in the brains was extracted with 500 μl formamide for 24 h at 38°C. The amount of EB in the supernatants was measured against 90% formamide solution in saline at 630 nm using a plate reader (Multiscan Ascent; Thermo Labsystems, Franklin, MA, USA). EB levels were expressed as ng/g of brain tissue against a standard curve.

The determination of plasma cytokine concentrations
Whole blood was taken into blood collection tubes containing EDTA (Terumo Medical, Elkton, MD, USA). Supernatant plasma was separated by centrifugation at 3500 × *g* for 2 min and frozen under −80°C until assayed for cytokines. The analysis of plasma cytokine levels was conducted using a mouse inflammation cytometric bead array kit and a FACSArray bioanalyzer (Becton Dickinson, USA) (Li *et al*, 2007; Morgan *et al*, 2004). The experiment was conducted following manufacturer's instructions. Standard curves were determined for each cytokine

from the range of 20 to 5000 pg/ml. The following cytokines were measured: IL-6, IL-10, MCP-1, IFN-γ, TNF-α, and IL-12p70.

Plaque assay

To evaluate viral titer, we performed a plaque assay as previously described (Tsuda *et al*, 2009). Briefly, Mardin-Darby canine kidney (MDCK) cells were grown in Eagle's minimal essential medium (EMEM; Nissui Pharmaceutical, Tokyo, Japan) supplemented with 10% inactivated fetal bovine serum and 2 mM L-glutamine. Pieces of mouse tissues were homogenized in 10% concentration with EMEM under 4°C. The 10-fold dilutions of the homogenized sample were inoculated to confluent monolayers of MDCK cells and incubated for 1 h at 37°C. The dilutions were removed, and the cells were washed with PBS. Cells were overlaid with EMEM containing 1% Bacto Agar (Becton Dickinson) and 0.0005% acetyl trypsin. After 48 h of inoculation at 37°C, cells were stained with 0.005% neutral red for 12 h and visible plaques were counted.

Declaration of interest: The authors report no conflicts of interest. The authors alone are responsible for the content and writing of the paper.

References

Aiba H, Mochizuki M, Kimura M, Hojo H (2001). Predictive value of serum interleukin-6 level in influenza virus-associated encephalopathy. *Neurology* **57:** 295–299.

Alexander J, Jacob A, Cunningham P, Hensley L, Quigg R (2008). TNF is a key mediator of septic encephalopathy acting through its receptor, TNF receptor-1. *Neurochem Int* **52:** 447–456.

Bigdeli M, Khoshbaten A (2008). In vivo preconditioning with normobaric hyperoxia induces ischemic tolerance partly by triggering tumor necrosis factor-alpha converting enzyme/tumor necrosis factor-alpha/nuclear factor-kappaB. *Neuroscience* **153:** 671–678.

Bogdanski R, Blobner M, Becker I, Hänel F, Fink H, Kochs E (2000). Cerebral histopathology following portal venous infusion of bacteria in a chronic porcine model. *Anesthesiology* **93:** 793–804.

Fukui S, Fazzina G, Amorini AM, Dunbar JG, Marmarou A (2003). Differential effects of atrial natriuretic peptide on the brain water and sodium after experimental cortical contusion in the rat. *J Cerebr Bood F Met* **23:** 1212–1218.

Han J, Brown T, Beutler B (1990). Endotoxin-responsive sequences control cachectin/tumor necrosis factor biosynthesis at the translational level. *J Exp Med* **171:** 465–475.

Ichiyama T, Isumi H, Ozawa H, Matsubara T, Morishima T, Furukawa S (2003). Cerebrospinal fluid and serum levels of cytokines and soluble tumor necrosis factor receptor in influenza virus-associated encephalopathy. *Scand J Infect Dis* **35:** 59–61.

Isoda N, Sakoda Y, Kishida N, Bai G, Matsuda K, Umemura T, Kida H (2006). Pathogenicity of a highly pathogenic avian influenza virus, A/chicken/Yamaguchi/7/04 (H5N1) in different species of birds and mammals. *Arch Virol* **151:** 1267–1279.

Ito Y, Ichiyama T, Kimura H, Shibata M, Ishiwada N, Kuroki H, Furukawa S, Morishima T (1999). Detection of influenza virus RNA by reverse transcription-PCR and proinflammatory cytokines in influenza-virus-associated encephalopathy. *J Med Virol* **58:** 420–425.

Jakeman K, Rushton D, Smith H, Sweet C (1991). Exacerbation of bacterial toxicity to infant ferrets by influenza virus: possible role in sudden infant death syndrome. *J Infect Dis* **163:** 35–40.

Julkunen I, Melén K, Nyqvist M, Pirhonen J, Sareneva T, Matikainen S (2000). Inflammatory responses in influenza A virus infection. *Vaccine* **19**(Suppl 1): S32–S37.

Kawai T, Akira S (2006). TLR signaling. *Cell Death Differ* **13:** 816–825.

Li Z, Hulderman T, Salmen R, Chapman R, Leonard S, Young S, Shvedova A, Luster M, Simeonova P (2007). Cardiovascular effects of pulmonary exposure to single-wall carbon nanotubes. *Environ Health Perspect* **115:** 377–382.

Lundemose J, Smith H, Sweet C (1993). Cytokine release from human peripheral blood leucocytes incubated with endotoxin with and without prior infection with influenza virus: relevance to the sudden infant death syndrome. *Int J Exp Pathol* **74:** 291–297.

Matsuda K, Park C, Sunden Y, Kimura T, Ochiai K, Kida H, Umemura T (2004). The vagus nerve is one route of transneural invasion for intranasally inoculated influenza A virus in mice. *Vet Pathol* **41:** 101–107.

Morgan E, Varro R, Sepulveda H, Ember J, Apgar J, Wilson J, Lowe L, Chen R, Shivraj L, Agadir A, Campos R, Ernst D, Gaur A (2004). Cytometric bead array: a multiplexed assay platform with applications in various areas of biology. *Clin Immunol* **110:** 252–266.

Morishima T, Togashi T, Yokota S, Okuno Y, Miyazaki C, Tashiro M, Okabe N, (2002). Encephalitis and encephalopathy associated with an influenza epidemic in Japan. *Clin Infect Dis* **35:** 512–517.

Nain M, Hinder F, Gong J, Schmidt A, Bender A, Sprenger H, Gemsa D (1990). Tumor necrosis factor-alpha production of influenza A virus-infected macrophages and potentiating effect of lipopolysaccharides. *J Immunol* **145:** 1921–1928.

Okita K, Tokino T, Nishimori H, Miura K, Nikaido H, Hayakawa J, Ono A, Kuwajima M, Matsuzawa Y, Nakamura Y (1996). Definition of the locus responsible for systemic carnitine deficiency within a 1.6-cM region of mouse chromosome 11 by detailed linkage analysis. *Genomics* **33:** 289–291.

Papadopoulos M, Davies D, Moss R, Tighe D, Bennett E (2000). Pathophysiology of septic encephalopathy: a review. *Crit Care Med* **28:** 3019–3024.

Smidt MH, Stroink H, Bruinenberg JFM, Peeters M (2004). Encephalopathy associated with influenza A. *Eur J Paediatr Neurol* **8:** 257–260.

Stolp H, Dziegielewska K, Ek C, Habgood M, Lane M, Potter A, Saunders N (2005). Breakdown of the blood-brain barrier to proteins in white matter of the developing brain following systemic inflammation. *Cell Tissue Res* **320:** 369–378.

Togashi T, Matsuzono Y, Narita M, Morishima T (2004). Influenza-associated acute encephalopathy in Japanese children in 1994–2002. *Virus Res* **103:** 75–78.

Toovey S (2008). Influenza-associated central nervous system dysfunction: a literature review. *Travel Med Infect Dis* **6:** 114–124.

Tsuda Y, Isoda N, Sakoda Y, Kida H (2009). Factors responsible for plaque formation of A/duck/Siberia/272/1998 (H13N6) influenza virus on MDCK cells. *Virus Res* **140:** 194–198.

Yao D, Chen Y, Kuwajima M, Shiota M, Kido H (2004). Accumulation of mini-plasmin in the cerebral capillaries causes vascular invasion of the murine brain by a pneumotropic influenza A virus: implications for influenza-associated encephalopathy. *Biol Chem* **385:** 487–492.

Yokota S, Imagawa T, Miyamae T, Ito S, Nakajima S, Nezu A, Mori M (2000). Hypothetical pathophysiology of acute encephalopathy and encephalitis related to influenza virus infection and hypothermia therapy. *Pediatr Int* **42:** 197–203.

This paper was first published online on Early Online on 29 March 2010.